Chapter

A Constant Gain Kalman Filter for Wireless Sensor Network and Maneuvering Target Tracking

Peeyush Awasthi, Ashwin Yadav, Naren Naik and Mudambi Ramaswamy Ananthasayanam

Abstract

One of the well-known approaches to target tracking is the Kalman filter. The problem of applying the Kalman Filter in practice is that in the presence of unknown noise statistics, accurate results cannot be obtained. Hence the tuning of the noise covariances is of paramount importance in order to employ the filter. The difficulty involved with the tuning attracts the applicability of the concept of Constant Gain Kalman Filter (CGKF). It has been generally observed that after an initial transient the Kalman Filter gain and the State Error Covariance P settles down to steady state values. This encourages one to consider working directly with steady state or constant Kalman gain, rather than with error covariances in order to obtain efficient tracking. Since there are no covariances in CGKF, only the state equations need to be propagated and updated at a measurement, thus enormously reducing the computational load. The current work first applies the CGKF concept to heterogeneous sensor based wireless sensor network (WSN) target tracking problem. The paper considers the Standard EKF and CGKF for tracking various manoeuvring targets using nonlinear state and measurement models. Based on the numerical studies it is clearly seen that the CGKF out performs the Standard EKF. To the best of our knowledge, such a comprehensive study of the CGKF has not been carried out in its application to diverse target tracking scenarios and data fusion aspects.

Keywords: Constant Gain Kalman Filter, INS, GPS, Wireless Sensor Network, Tracking

1. Introduction

The Kalman Filter (KF) is one of the most fundamental and widely used estimation schemes in tracking application. While the KF formalism is very powerful we need to keep in mind that the solution scheme can be considered to be formal and a fundamental prerequisite for accurate results is the a prioiri knowledge of the initial state (X_0), initial state noise covariance (P_0), system noise covariance (Q), measurement noise covariance (R). Good values of X_0, P_0, Q and R are imperative for the filter to perform optimally. Tuning of the KF is defined as the process to obtain precise values of P_0, Q, and R. A detailed review of filter tuning has been given by Ananthasayanam et al. in [1]. A main theme of filter covariance tuning schemes is the notion of the innovation sequence being white and Gaussian for filter optimality.

One class of schemes obtains the unknown covariances that maximize the likelihood [2–5]. Another important class of filter covariance tuning schemes is the covariance matching methodology [6–8]. The idea of an innovations based cost function being minimized by the optimal covariances is also used in [7, 8] to tune process system noise (Q) and state error covariances (P) respectively.

An alternate approach to tuning is via the direct setting of the Kalman gain as carried out in the work of Ananthasayanam et al. [9] and Ashwin et al. [10]. It is often observed that the Kalman gain converges to a steady state value which coincides with the convergence of the state error covariance P. The premise for working with the steady state or constant gain is well explained in the thesis work by Bohn [11]. The work of Anil Kumar et al. [9], optimizes the innovations likelihood cost function [5] for the (constant) Kalman gain in a space craft reentry problem. This CGKF approach works directly with the Kalman gain and does not utilize any knowledge of the filter covariances.

Our present work is about the application and sensitivity study of the CGKF traget tracking scheme in sensor networks scenarios and maneuvering target tracking. We look at target tracking problems in wireless sensor networks using passive infrared (PIR), acoustic and seismic sensors in stand alone (SA) and data fusion (DF) modes as given by Raol [12] for the discrete white noise acceleration (DWNA) traget motion model. We further demonstrate the capability of the CGKF to track maneuvering targets [13, 14] from acquired range and direction data for a class of coordinated turn (CT) maneuver models. The CGKF with linear measurement model was validated in [10, 15]. The present study applies the CGKF to a non linear measurement models and further demonstrates its robustness through sensitivity studies. The results obtained with respect to homogeneous and heterogeneous data fusion further demonstrate the range of applicability of the CGKF. These extensive tracking and sensitivity studies for a wide range of state and measurement models are to the best of our knowledge, unique to this paper and provide the reader with a comprehensive reference. These results also provide a firm base for application of the CGKF concept to other areas. In the sequel, Section 2 describes the CGKF concept. Section 3 introduces the various tracking scenarios based on PIR, acoustic and seismic measuerement models in SA and DF modes. In addition maneuvering targets based on CT models are discussed, since these have the potential to demonstrate the flexibility of the CGKF. Section 4 details the tracking and sensitivity studies on the above mentioned models, and Section 5 gives the conclusion of the present work.

2. Constant gain Kalman filtering

The KF algorithm [16] is based on the least squares principle with recursive time updates. It is a fact that optimal filter performance needs apriori knowledge of the filter statistics in terms of the state-error, system and measurement noise covariances (P, Q and R respectively). A central theme in the optimality of the KF is the requirement of the innovations being white at convergence [17, 18]. Mehra [17] shows that the settling of the filter gain value to a steady state value coincides with the state error covariance also similarly settling (**Figure 1**).

The observation that the gain (reflecting P, Q, R) reaches a steady state, prompts us to consider working directly with the steady state gain rather than the tuning dependant P, Q, R matrices to determine the gain. The way we accomplish this is via an innovations cost function minimization approach. We use the whiteness of the innovations at KF convergnce in order to construct the likelihood based function of the innovations sequence [5].

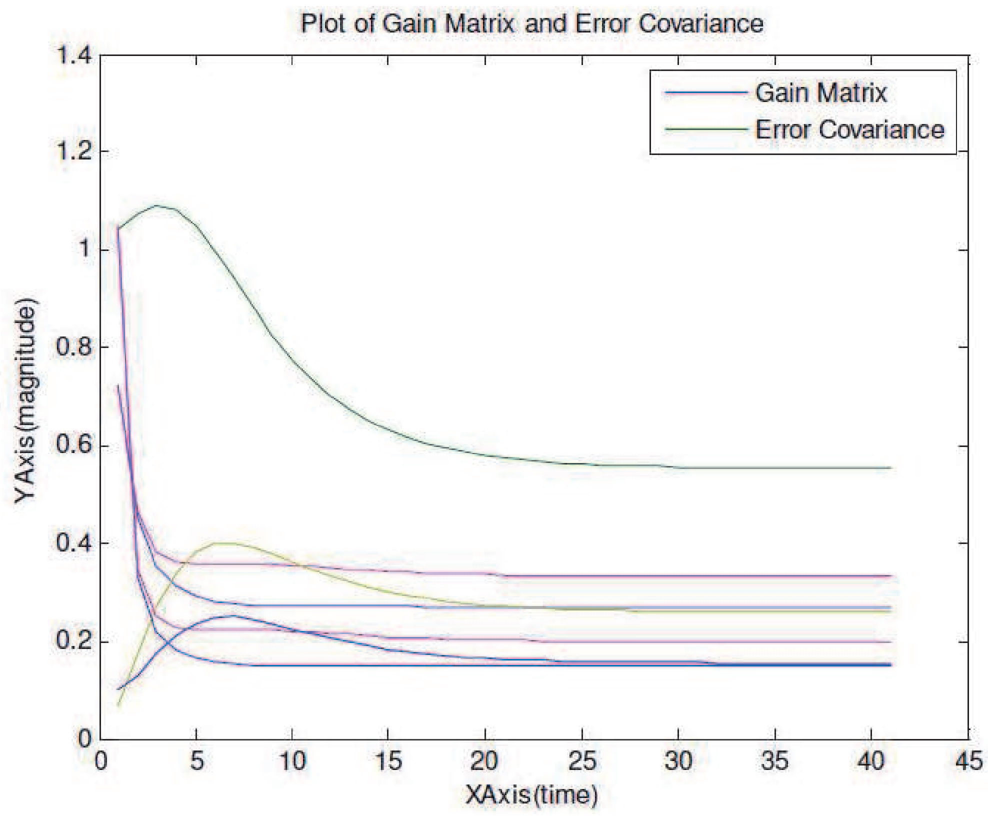

Figure 1.
Gain K *vs. error covariance matrix* P.

$$J(K, \mathcal{R}) = \frac{1}{N} \sum_{t=1}^{N} \left(v_t^T \mathcal{R} v_t + log\left(|\mathcal{R}|\right) \right) \tag{1}$$

where v_t represents the innovations, $\mathcal{R}$ represents the innovations covariance, $|.|$ represents the determinant and N is the number of measurement time steps. We obtain the steady state gain K^* and innovation covariance $\mathcal{R}^*$ by solving the following optimization problem

$$(K^*, \mathcal{R}^*) = argmin_{K,\mathcal{R}} J(K, \mathcal{R}) \tag{2}$$

The following is the estimation scheme based on a predict and update mode.

2.1 The estimation scheme

The generic KF updates are

$$\hat{x}_t = \overline{x}_t + K_t v_t \tag{3}$$

where the the innovations sequence is $v_t = y_t - C\overline{x}_t$. C is the measurement matrix, $\overline{x}_t$ is the predicted state matrix and $\hat{x}_t$ is the filtered state matrix. The standard KF computes the gain matrix K_t using P, Q and R while we proceed to estimate this constant gain K^* for the CGKF, by solving the optimization problem described by (2) above. The optimization problem can be solved using local gradient based methods (such as Newton type schemes) [19] or global schemes such as Genetic Algorithm (GA) [20] applied to problems as in [9]. As the filter tracks the target, the gain K is seen to stabilize to a value given by the solution of the above problem. Once we have computed the optimal filter gain K_t (denoted henceforth by K^*, representative of the constant gain) for the CGKF, the KF recursions become.

Predict

$$\bar{x}_{t+1} = A\hat{x}_{t+1} + u_{t+1} \tag{4}$$

Update

$$\hat{x}_{t+1} = \bar{x}_{t+1} + K^* \left(y_{t+1} - C\bar{x}_{t+1}\right) \tag{5}$$

Thus it is evident that once the optimal gain K^* is computed using GA to solve the optimization problem, the filter algorithm reduces to a simple predict and update model given by (4) and (5) above. This is obviously more compact compared to the standard KF which is implemented in five steps involving computation and propagation of the State Error Covariance P using Q and R. The advantage is speed of operation because we circumvent the tedious calculations of the costly covariance matrices P, Q, R and instead work directly with the optimal gain for the set of measurements.

We observe that the typically expensive covariance time update step is not needed in the constant gain approach.The CGKF is found to work quite well even with state models moderately different from that for which the gains are computed [25], suggesting a robustness of the gains calculated (Refer **Tables 6** and 7). It is to be noted that the present problem is a non linear problem, in so far as the measurement model is concerned so that the filter used is the CGKF. This is one unique advantage of the CGKF over the standard KF/EKF wherein the EKF requires linearization of the measurement model via use of the Jacobian H. The reconstruction in CGKF case employing the GA as the optimization tool, does not rely on the Jacobian in computation of the optimum Constant Filter Gain K^*.

3. Sensor models and modes

The focus of our study is the application of the CGKF to a variety of 2D sensor models such as those in unattended ground sensor (UGS) and Intelligence, Surveillance and Reconnaissance (ISR) systems. Sensors such as passive infrared (PIR) [21], acoustic, seismic [22] and radar have been studied. The sensor system might consist of single or multiple data inputs as required in different scenarios. They may consist of single type of sensor or multiple type of sensor nodes, as required in situations. Homogeneous and heterogeneous DF aspects of certain combination of sensors will be analyzed. We outline the regular and CGKF schemes and their application to the above mentioned systems.

3.1 State variable models in stand alone mode

Non Maneuvering or Discrete White Noise Acceleration (DWNA) Model.

The state model for 2D target is comprised of x and y direction displacement and their corresponding velocities wherein the state vector is represented as $X_t = \left[x_t, y_t, \dot{x}_t, \dot{y}_t\right]^t$ with x_t, y_t representing X,Y coordinates respectively of the target and $\dot{x}_t, \dot{y}_t$ representing velocities in X, Y directions.

State Equation.

The state equation for the DWNA is

$$X_{t+1} = AX_t + Bw_t \tag{6}$$

where

$$A = \begin{pmatrix} 1 & 0 & T_s & 0 \\ 0 & 1 & 0 & T_s \\ 0 & 0 & 1 & 0 \\ 0 & 0 & 0 & 1 \end{pmatrix}, B = \begin{pmatrix} 0.5T_s^2 & 0 \\ 0 & 0.5T_s^2 \\ T_s & 0 \\ 0 & T_s \end{pmatrix} \tag{7}$$

with A and B being the state - transition and acceleration matrices respectively, w_t being an uncorrelated Gaussian process.

Measurement equation: The measurement at time t of n^{th} sensor $g_t^{(n)}$

$$g_t^{(n)} = h^{(n)}(X_t, t) + v_t^{(n)} \tag{8}$$

where $h^{(n)}(X_t, t)$ is typically a nonlinear function of the states $v^{(n)}$ is the corresponding measurement noise (assumed to be white Gaussian) of n^{th} sensor. The measurement equations for the respective sensors are given below.

Sensor Measurement model for PIR sensor [21]

$$g_t^{(n)} = log \frac{\dot{x}_t^2 + \dot{y}_t^2}{\left(x_t - r_x^{(n)}\right)^2 + \left(y_t - r_y^{(n)}\right)^2} + v_t^{(n)} \tag{9}$$

Sensor Measurement model for Acoustic sensor [22]

$$g_t^{(n)} = tan^{-1}\left(y_t - r_y^{(n)}/x_t - r_x^{(n)}\right) + v_t^{(n)} \tag{10}$$

Sensor Measurement model for Seismic sensor [22]

$$g_t^{(n)} = \begin{pmatrix} \left(\left(x_t - r_x^{(n)}\right)^2 + \left(y_t - r_y^{(n)}\right)^2\right)^{0.5} + v_t^{(n)} \\ tan^{-1}\left(y_t - r_y^{(n)}/x_t - r_x^{(n)}\right) + v_t^{(n)} \end{pmatrix} \tag{11}$$

where $r^{(n)} = \left[r_x^{(n)}, r_y^{(n)}\right]$ is the position of the n^{th} sensor in network.

Estimation Scheme.

We now outline the estimation scheme by an EKF as well as a CGKF. The EKF has the following steps. For t = 0,1,2......

Prediction

$$\overline{X}_{t+1} = A\hat{X}_t \tag{12}$$

$$\overline{P}_{t+1} = A\hat{P}_t A' + Q \tag{13}$$

where $\overline{X}_{t+1}$ is the predicted estimate based on the filtered estimate $\hat{X}_t$, where $\overline{P}_{t+1}$ and $\hat{P}_t$ being the state error covariances corresponding to the predicted $\overline{X}_{t+1}$ and filtered $\hat{X}_t$ estimates respectively. and $Q = BE(ww')B'$.

Update/Correction: The update of the states and covariances as per the EKF scheme are

$$\hat{X}_{t+1} = \overline{X}_{t+1} + K_{t+1}\left(g_{t+1} - h\left(\overline{X}_{t+1}, t\right)\right) \tag{14}$$

where

$$K_{t+1} = \overline{P}_{t+1} H_{t+1}{}' \left(H_{t+1} \overline{P}_{t+1} H_{t+1}{}' + R \right)^{-1} \tag{15}$$

where H_{t+1} is the Jacobian corresponding to $h(.)$ at time $t+1$ and $R = E(vv')$.

$$\hat{P}_{t+1} = (I - K_{t+1} H_{t+1}) \overline{P}_{t+1} \tag{16}$$

Table 1 gives measurement Jacobians for all three sensors. In the table $\overline{d}_t = \left(\overline{x}_t - r_x^{(n)} \right)^{\overline{2}} + \left(\overline{y}_t - r_y^{(n)} \right)^2$ is used for sake of brevity of space.

The CGKF on the other hand has the following two steps.

Prediction

$$\overline{X}_{t+1} = A \hat{X}_{t+1} \tag{17}$$

Update/Correction.

Once the optimized Kalman gain K has been calculated via equations - 1,2 The following Eq. (17) updates the state parameters.

$$\hat{X}_{t+1} = \overline{X}_{t+1} + K\left(g_{t+1} - h\left(\overline{X}_t, t \right) \right) \tag{18}$$

In our work the optimized value of K is calculated via the application of the genetic algorithm to the innovation cost function Eqs. (1) and (2).

3.2 Homogeneous data fusion

In homogeneous fusion the fusion is based on the data from multiple sensors of similar type, at every time instant. Here in this section we have used mainly the centralized approach to DF in respect of the KF. The data obtained from various nodes (similar type of sensors) is combined together then applied to EKF and CGKF for tracking the target. This approach has been used as measurement fusion [12] approach in WSN of UGSs.

Measurement fusion techniques combine the raw measurements of the target obtained from the Individual Sensor Node (ISN) at the Cluster Head Node (CHN) Level. The ISN is a tier 1 node while the CHN is a tier 2 node which is capable of running a complex fusion algorithm based on KF framework. So ISNs are considered to have minimal computation capability compared to the CHNs. The two approaches which have been implemented in our work with respect to the CGKF under the

Sensors Type	Measurement Equation	Jacobian H
PIR	$h = log \frac{\overline{x}_t^2 + \overline{y}_t^2}{\left(\overline{x}_t - r_x^{(n)}\right)^2 + \left(\overline{y}_t - r_y^{(n)}\right)^2}.$	$H = \left[\frac{-2\left(\overline{x}_t - r_x^{(n)}\right)}{\overline{d}^2{}_t}, \frac{-2\left(\overline{y}_t - r_y^{(n)}\right)}{\overline{d}_t{}^2}, \frac{2\overline{x}_t}{\overline{x}_t^2 + \overline{y}_t^2}, \frac{2\overline{y}_t}{\overline{x}_t^2 + \overline{y}_t^2} \right]$
ACO-USTIC	$h = tan^{-1}\left(y_k - r_y^{(n)} / x_k - r_x^{(n)} \right)$	$H = \left[\frac{\left(r_y^{(n)} - \overline{y}_t\right)}{\overline{d}t}, \frac{\overline{x}_t - r_x^{(n)}}{\overline{d}_t}, 0, 0 \right]$
SEISMIC	$h = \begin{pmatrix} \left(\left(x_t - r_x^{(n)} \right)^2 + \left(y_t - r_y^{(n)} \right)^2 \right)^{0.5} + v_t^{(n)} \\ tan^{-1}\left(y_t - r_y^{(n)} / x_t - r_x^{(n)} \right) + v_t^{(n)} \end{pmatrix}$	$H = \left[\frac{\overline{x}_t - r_x^{(n)}}{\overline{d}_t^{0.5}}, \frac{\overline{y}_t - r_y^{(n)}}{\overline{d}_t^{0.5}}, 0, 0; \frac{\left(r_y^{(n)} - \overline{y}_t\right)}{\overline{d}_t}, \frac{\left(r_x^{(n)} - \overline{x}_t\right)}{\overline{d}_t}, 0, 0 \right]$

Table 1.
Jacobians for sensors measurement models.

homogeneous DF are Maximal Kalman filter (MKF) [12] and Weighted fusion (WF) [12] approaches. The state model is the DWNA model of the previous sub section.

3.2.1 Maximal Kalman filter (MKF) method

This method is based on fusing all measurements of the ISN by incorporating them in a fused measurement vector and the corresponding measurement noise covariance and measurement matrices as described below

$$g_t^f = \left[g_t^1, g_t^2, \ldots \ldots g_t^m\right] \tag{19}$$

$$H_t^f = \left[H_t^1, H_t^2, \ldots \ldots H_t^m\right] \tag{20}$$

$$R_t^f = diag\left[R_t^1, R_t^2, \ldots \ldots R_t^m\right] \tag{21}$$

where g_t^f in (16) is the fused measurement vector, by combining the measurements of m sensors (ISNs) at time instant t. Similarly H_t^f is the corresponding value of the Jacobian of the respective ISNs. In (21) R_t^f is the measurement error covariance. Note that no modification measurements of the ISNs is carried out here and pure measurements of the target are being fused at the CHN to obtain the final state vector and state error covariance.

3.2.2 WF method

This method is based on combining the m measurements in a different manner than MKF. A weighing factor ϖ is allotted to each of the corresponding measurements of the ISNs, which represents the degree of correctness or confidence that one has regarding the measurement obtained from a specific ISN. The weight factor has been applied to Eqs. (19)–(21) as follows

$$g_t = \frac{\sum_{m=1}^{N}\left(\varpi_t^m g_t^m\right)}{\sum_{m=1}^{N} w_t^m} \tag{22}$$

$$H_t = \frac{\sum_{m=1}^{N}\left(\varpi_t^m H_t^m\right)}{\sum_{m=1}^{N} w_t^m} \tag{23}$$

$$R_t = \frac{\sum_{m=1}^{N}\left(\varpi_t^m R_t^m\right)}{\sum_{m=1}^{N} \varpi_t^m} \tag{24}$$

where g_t, H_t and R_t are the composite measurement vector, measurement-matrix/Jacobian and measurement noise covariance matrix respectively obtained by combining respective components from the m sensors sensing the target at that specific time instant. The ϖ_t^m is the weight alotted to the m^{th} sensor at t^{th} time instant. Possible choices for the weights are

$$\varpi_t^m = \frac{1}{R_t^m} \tag{25}$$

$$\varpi_t^m = \frac{1}{\left(d_t^m\right)^r} \tag{26}$$

where R_t^m represents the measurement noise of the m^{th}sensor, d_t^m the distance of the m^{th} sensor from the target and r represents the path loss exponent. In our simulations we have used Eq. (25). We utilize the above weighted - fused quantities in the EKF and the CGKF.

3.3 Heterogeneous DF

Heterogeneous DF differs from the homogeneous variety in that we fuse data from different types of sensors in combinations: such as, PIR and acoustic or PIR and seismic or PIR, acoustic and seismic together [12]. We have tried the architectures of centralized (measurement fusion) as well as decentralized (state fusion) data fusion. There are several methods in practice for DF but for nonlinear measurement models, it has been found that only a few models have been able to maintain the accuracy against catastrophic fusion [23]. The state model applied is the DWNA (Eq. (6)) of the subsection A.

3.3.1 Centralized DF

This architecture mainly follows the measurement fusion. The measurements (data) are obtained from all ISNs and then fused at cluster head node CHNs. In our case the data obtained is nonlinear from all three sensors with different size of measurement models. The only possible approach to collate data effectively is the MKF since weighted fusion applies only to sensors based on similar measurement model. The method has been applied to both EKF and CGKF.

The MKF is an effective way to combine data from dissimilar type of sensor measurement models. At the cost of computational complexity owing to matrix size this is overall an effective method considering WF can combine data from only similar group of sensors.

3.3.2 Decentralized data fusion

The method has been explicitly used to bring out the fact the CGKF did perform better as against any of these methods of combining state parameters and covariances. This method has been cited as state fusion concept [12] or hierarchical data fusion. This is based on a two tier system wherein state estimation of the target is carried out at ISNs which forms tier 1 and these states are then fused at tier 2 in the CHNs. The global state estimate and global state error covariance calculated at CHNs and these are then fed to ISNs. The KF algorithm runs in the ISN to obtain fresh state and error covariance estimates, which are again fed at the CHN and the cycle continues. There are mainly two approaches of track to track fusion as given by Raol [12] in Eq. (27) and (28) and Durrant whyte [24] in Eqs. (29) and (30). Most of the methods surveyed in this category feature a scheme where in we have to combine error covariances and state vectors to produce new covariance and state vectors. The only difference between the two methods below is the way state estimates and error covariances are used to compute fused global values of state estimate $\overline{X}_{t+1}^{f}$ and state error covariance $\overline{P}_{t+1}^{f}$ at $t+1$ time instant. The symbols used in the equations below $P^1$and P^2 are the covariances with respect to two different sensors. $\hat{X}_t^1$ and $\hat{X}_t^2$ are the target state vector as computed by the EKF at ISNs. $\overline{X}_{t+1}^{f}$ and $\overline{P}_{t+1}^{f}$ are the finally computed target state vector and state error covariances respectively at CHNs. This is fed back to every ISN after every iteration. In the present work we use the Global fusion method of Raol [12].

Global Fusion

$$\overline{X}^f_{t+1} = \hat{X}^1_t + \hat{P}^1_t \left(\hat{P}^1_t + \hat{P}^2_t\right)^{-1} \left(\hat{X}^2_t - \hat{X}^1_t\right) \tag{27}$$

$$\overline{P}^f_{t+1} = P^1_t - P^1_t \left(\hat{P}^1_t + \hat{P}^2_t\right)^{-1} P^{1T}_t \tag{28}$$

Track to Track Fusion

$$\overline{P}^f_{t+1} = \left[\sum_{i=1}^{N} P^{-1}_{i_t}\right]^{-1} \tag{29}$$

$$\overline{X}^f_{t+1} = \overline{P}^f_{t+1} \sum_{i=1}^{N} P^{-1}_{i_t} X_{i_t} \tag{30}$$

3.4 Maneuvering target

The class of maneuvering targets yield particularly challenging tracking problems. The challenges include choosing a system model close to the actual target maneuvers in addition to often having to give real time solutions. In our work we now aim to demonstarate the efficacy of the CGKF framework to RADAR- measurement based coordinated turn (CT) models. We reiterate that the non necessity of prior knowledge of the system and measurement noise characteristics (often representing the nature of maneuver) make the CGKF particularly attractive. The present work builds on [15] where the CGKF algorithm has been applied to a variety of maneuvering targets based on a linear measurement model. Currently a non linear measurement model (RADAR based) has been employed in order to move a step closer to a more realistic scenario. We have applied the CGKF to the highly maneuvering class of CT models with known as well as unknown turn rates [13, 14]. In the simulation studies the turn rate is represented by ω.

The present part is divided into the following parts.

3.4.1 CT state variable model

A two dimensional model for the target tracking problem (maneuver in horizontal 2D plane) is described as follows.

State Equation: CT known ω.

$$X_{t+1} = AX_t + Bw_t \tag{31}$$

where state vector is $X_t = (x(t)\ \ \dot{x}(t)\ \ y(t)\ \ \dot{y}(t))^T$, state transition matrix $A = \begin{pmatrix} A_1 & -A_2 \\ A_2 & A_1 \end{pmatrix}$, $B = \begin{pmatrix} B_1 & B_2 \\ B_2 & B_1 \end{pmatrix}$.

where $A_1 = \begin{pmatrix} 1 & Sin(\omega\Delta t)/\omega \\ 0 & Cos(\omega\Delta t) \end{pmatrix}$, $A_2 = \begin{pmatrix} 0 & (1 - Cos(\omega\Delta t))/\omega \\ 0 & Sin(\omega\Delta t) \end{pmatrix}$,

$B_1 = \begin{pmatrix} \Delta t^2/2 & 0 \\ \Delta t & 0 \end{pmatrix}$, $B_2 = \begin{pmatrix} 0 \\ 0 \end{pmatrix}$ and w_t represents system noise which is Gaussian and Δt is a time step. Here we have considered the state vector to include X and Y coordinates of the target as well as the speed in the two coordinates.

State Equation: CT with unknown ω

$$X_{t+1} = A(X_t)X_t + Bw_t \tag{32}$$

A two dimensional model for the target tracking problem (maneuver in horizontal 2D plane) is described as follows.

where state vector is $X_t = \begin{pmatrix} x(t) & \dot{x}(t) & y(t) & \dot{y}(t) & \omega(t) \end{pmatrix}^T$, state transition matrix $A(X_t) = \begin{pmatrix} A_1 & -A_2 & B_2 \\ A_2 & A_1 & B_2 \\ B_3 & B_3 & 1 \end{pmatrix}$, $B = \begin{pmatrix} \Delta t^2/2 & 0 & 0 \\ \Delta t & 0 & 0 \\ 0 & \Delta t^2/2 & 0 \\ 0 & 0 & \Delta t \\ 0 & 0 & \Delta t \end{pmatrix}$ where $B_3 = \begin{pmatrix} 0 & 0 \end{pmatrix}$, A_1,A_2,B_2,B_3 are as described above and w_t represents system noise which is white Gaussian. Inclusion of the angular speed ω in the state vector makes the state equation non linear for thecase of CT with unknown ω.

Measurement Equation:

$$g_t = \begin{pmatrix} \left(x(t)^2 + y(t)^2\right)^{.5} \\ tan^{-1}(y(t)/x(t)) \end{pmatrix} + v_t \tag{33}$$

where g_t is the measurement vector and v_t is measurement noise which is assumed to be white Gaussian.

4. Results and sensitivity studies

4.1 Stand alone mode

The tabulated result of all sensors for EKF and CGKF are given below with their respective PFE (Percentage Fit Error). The error metric $PFE = \frac{|X_t - \overline{X}_t|}{|X_t|} \times 100$ which represents the normalized difference between the estimated and actual track, achieved by CGKF and EKF. The PIR sensor gives the least error with CGKF. All the results in this section and subsequent sections are out of a minimum of 500 Montecarlo runs. The plots for EKF (Left) and CGKF (Right) have been combined together. The figures appear as top and bottom, top one is the true trajectory and bottom one is the true trajectory super imposed with estimated trajectory. The PFE is also mentioned on the graph itself for every case. This is same for all the cases given below.Where ever the error is negligible, the estimated track (green) completely takes over the actual track (black). Following are the deductions based on the simulation results. It is to be noted that the plots are based on one of the 500 runs used to compute the PFE metric (refer **Table 2**). This applies to the present and all subsequent sections also.One example of each sensor performance is displayed in the **Figures 2–4** respectively. The PFE, RMSPE metric (representative of the error in range calculation based on x, y coordinates of the target and expresssed as) in the plots correspond to that of the CGKF for a particular run.

Sensor Type	No of Sensors	EKF (PFE) %	CGKF (PFE) %
PIR	1	3.77076	1.03723
Acoustic	1	2.497723	1.9393
Seismic	1	4.622587	2.614668

Table 2.
Stand alone mode.

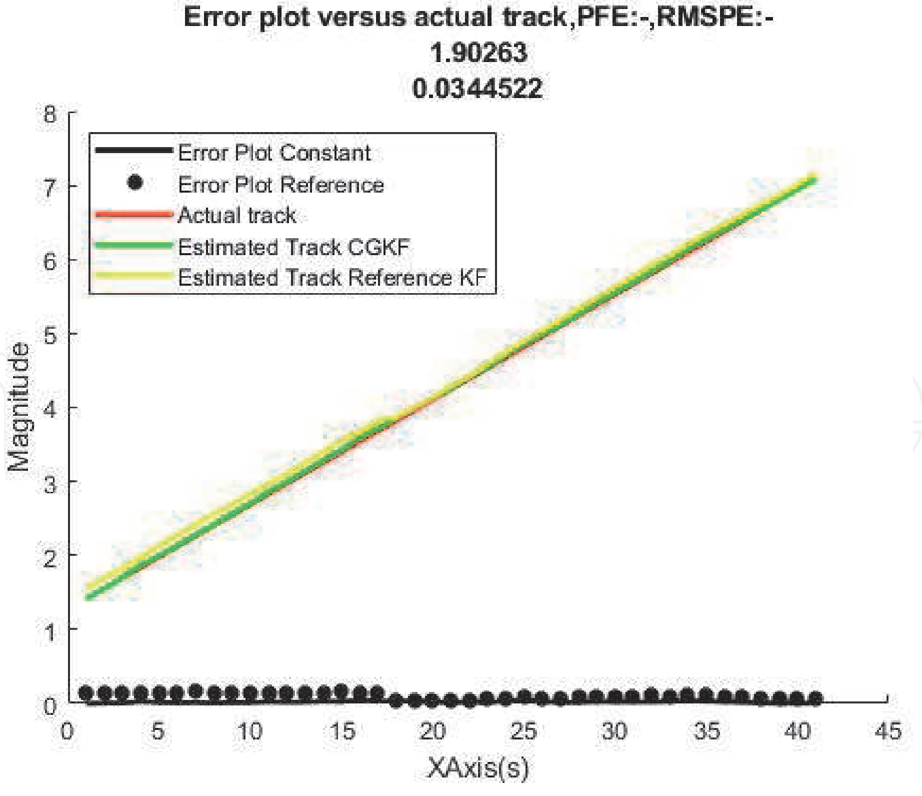

Figure 2.
Stand alone mode:-PIR sensor.

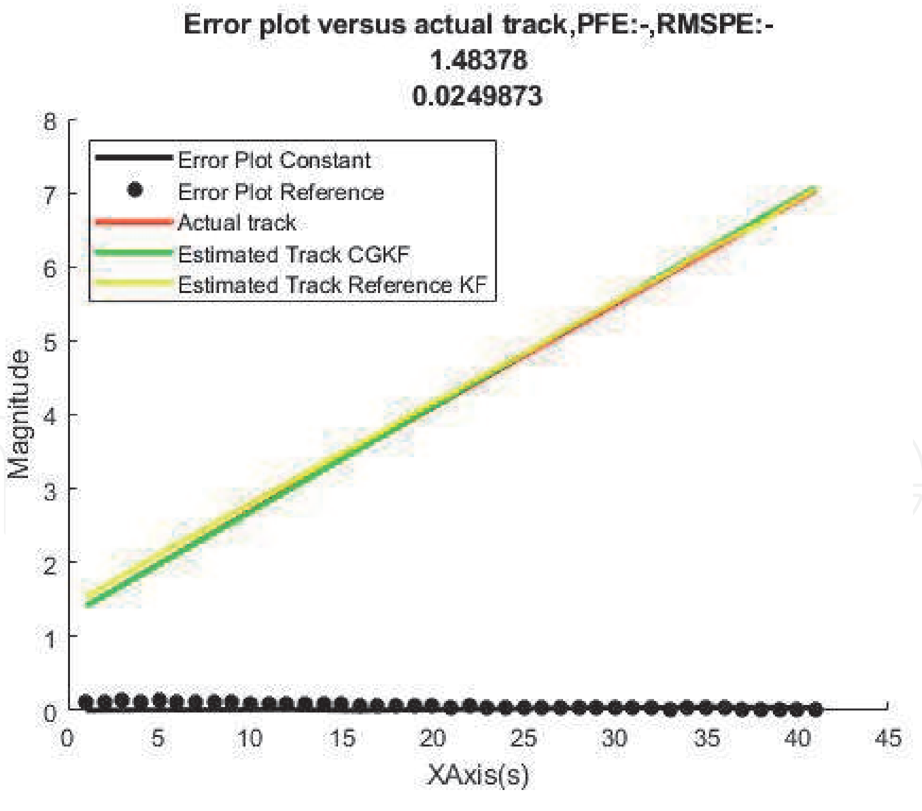

Figure 3.
Stand alone mode:-acoustic sensor.

4.2 Homogeneous fusion mode of sensors

The results from both, MKF and Weighted fusion have been tabulated seperately as shown in the first six enteries of **Table 3**. Settings of the simulations

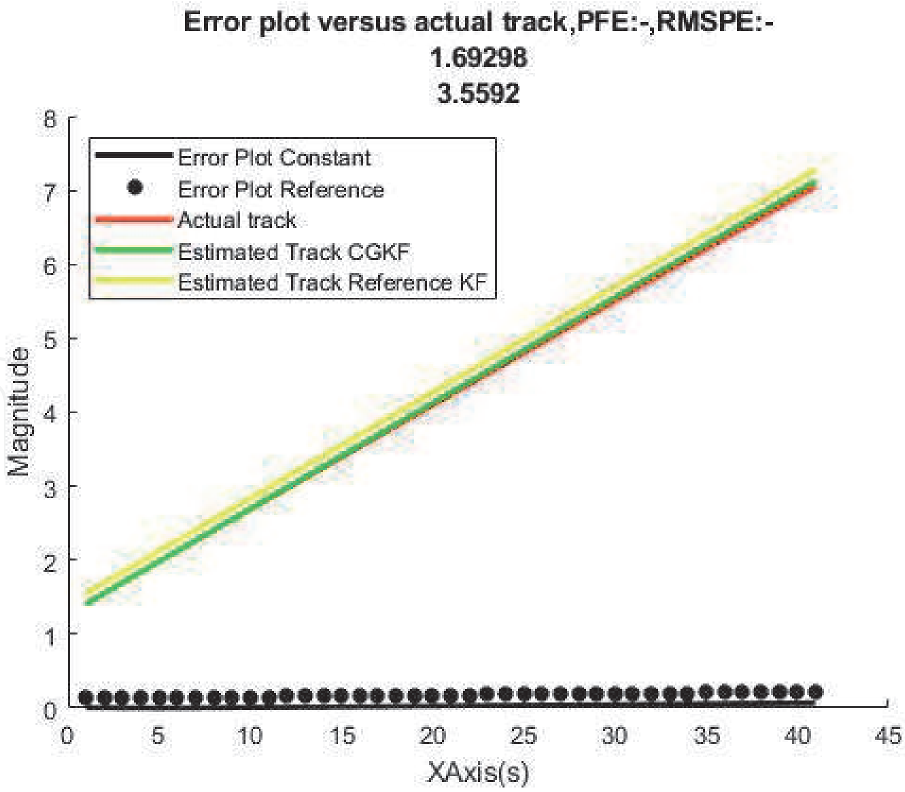

Figure 4.
Stand alone mode:- Sesimic sensor.

Sensor Type	EKF (PFE) %	CGKF (PFE)%	Fusion Type
PIR	6.32816	2.81109	Maximal
Acoustic	5.76208	5.61651	Maximal
Seismic	5.54418	2.38094	Maximal
PIR	0.580869	0.579842	Homogeneous Weighted
Acoustic	1.47602	1.33768	Homogeneous Weighted
Seismic	1.7170850	1.0956019	Homogeneous Weighted
PIR & Acoustic	18.5708	9.3724	Maximal
PIR, Acoustic & Seismic	19.9958	1.34023	Maximal
PIR & Seismic	10.9576	3.42436	Maximal

Table 3.
Measurement fusion:-4 sensor set.

including the number of Monte Carlo runs is same as that for the Stand Alone method described above. An example of the method is illustrated in **Figures 5** and **6**. The PFE, RMSPE metrics (as defined in Section 4.1) metric in the plots correspond to that of the CGKF for the coresponding run.

4.3 Heterogeneous fusion mode of sensors

The results in last three entries of **Table 3**, are those corresponding to the measurement fusion based method of heterogeneous fusion. Settings of the simulations including the number of Monte Carlo runs is same as that for the Stand Alone and homogeneous fusion method described above. One example each

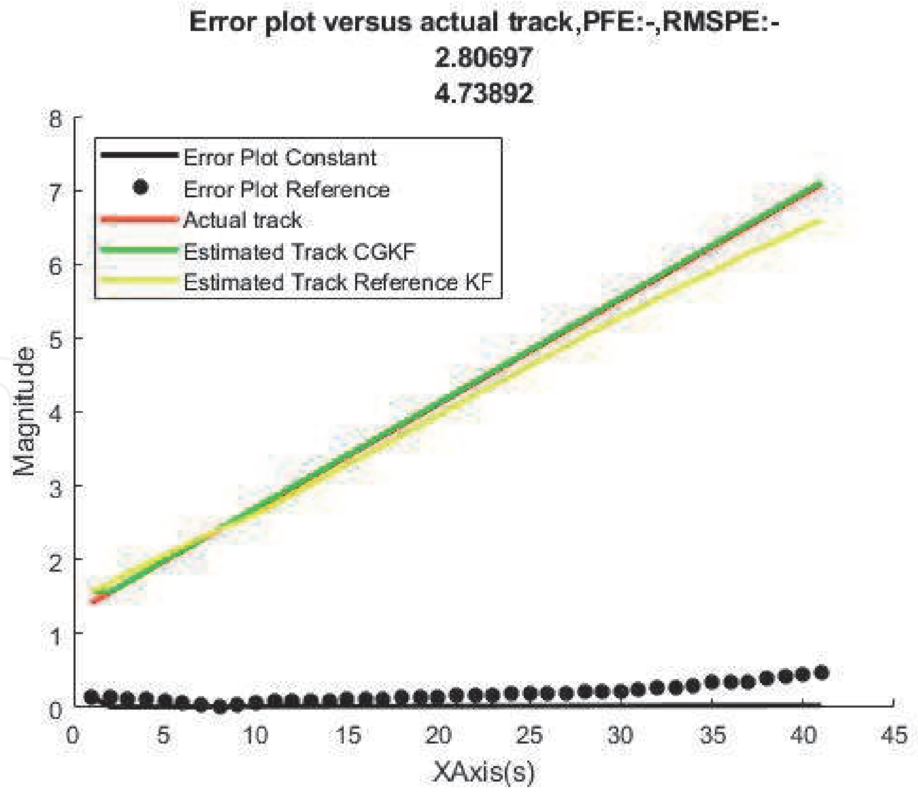

Figure 5.
Homogeneous fusion (MKF):- seismic sensor.

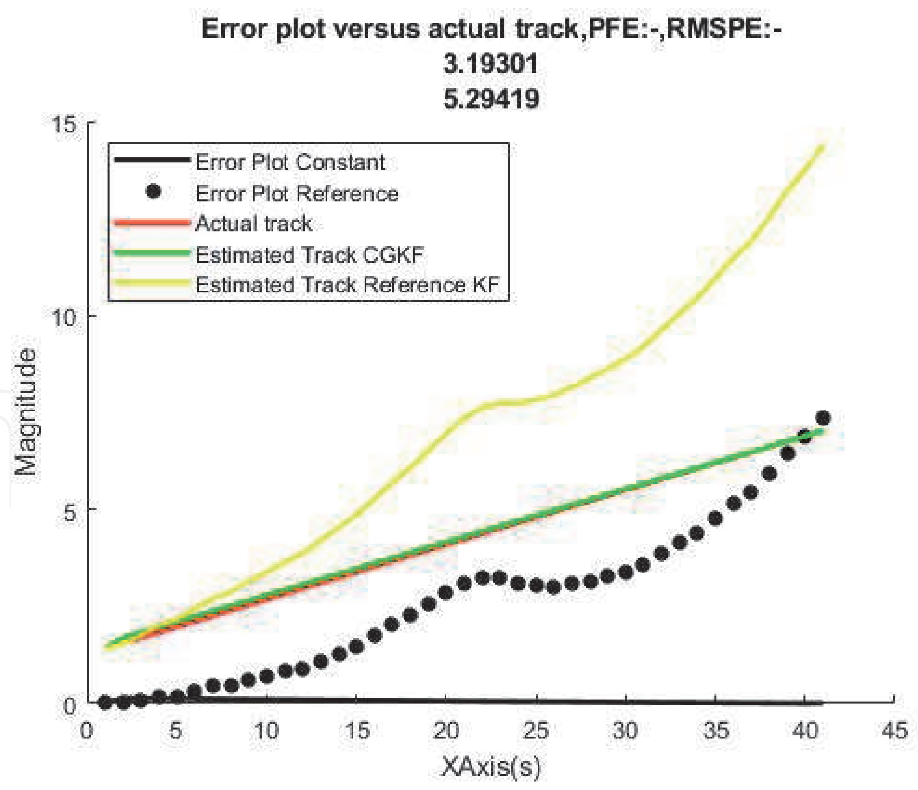

Figure 6.
Homogeneous fusion (weighted):- acoustic sensor.

of the two sensor (PIR and seismic case) and three sensor (all three combined) is illustrated in **Figures 7** and **8** repectively. The PFE, RMSPE metrics (as defined in Section 4.1) in the plots correspond to that of the CGKF for the coresponding run (refer **Table 4**).

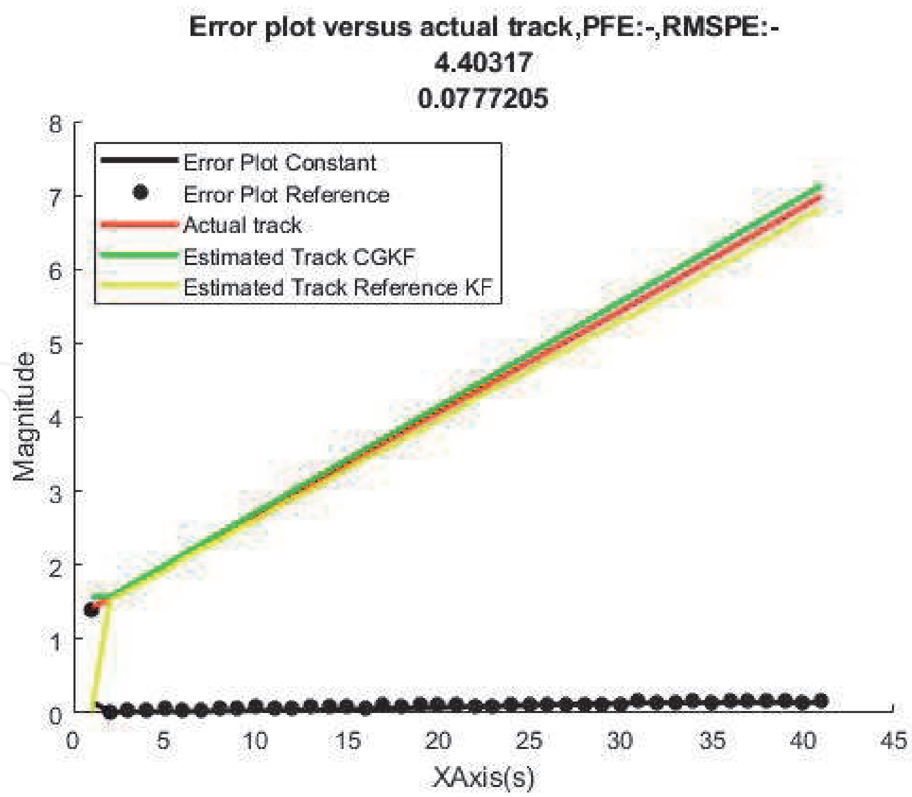

Figure 7.
Heterogeneous fusion (maximal):-PIR and seismic sensors.

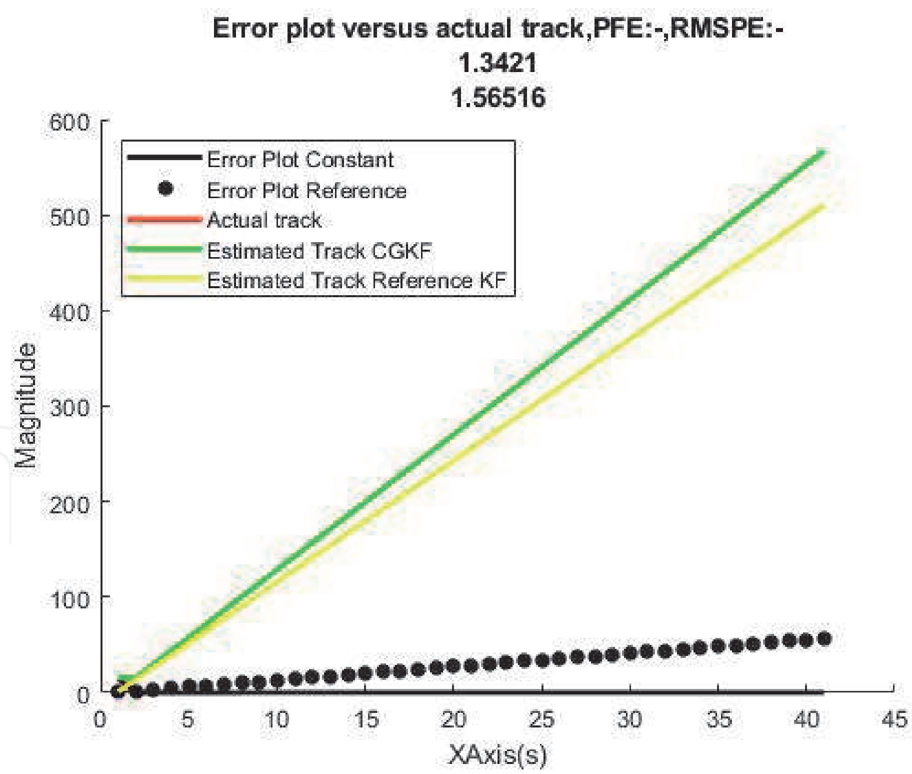

Figure 8.
Heterogeneous fusion (maximal):- PIR, seismic and acoustic sensors.

4.4 Maneuvering target

The 2-D frame work study has been carried out on a set of seventy data points in order to generate a smooth trajectory. The following system and measurement covariances matrices are used to generate the simulated track $Q = .01I$, $R = .1I$ for

Sensor Type	Fusion Type(State-Fusion)	EKF (PFE)%
PIR & Acoustic	Global Fusion [12]	2.29092
PIR, Acoustic & Seismic	Global Fusion [12]	NaN(Not a Number)*
PIR, Acoustic & Seismic	Whyte Method [24]	1.1158

:- Due to lack of convergence.

Table 4.
Heterogeneous fusion (state fusion).

all models, choice of the initial value of ω in the CT model has been obtained by via standard fighter aircraft (eg F-16) data available on the internet. This value of ω has been set to .5, which corresponds to approx 28.6 degrees/s (which happens to be the maximum instantaneous turn rate of any current generation fighter aircraft). Here the *PFE* is based on sum total *PFE* obtained along X and Y coordinates respectively. The error metric shown in tables is the average value computed over 500 runs while the plots correspond to one specific run wherein results are presented in the form of 2D plots of the simulated target trajectory, simulated measurements and the estimated track against time. **Table 5** shows the typical constant gain average values computed using GA over 500 runs corresponding to each of the models. Corresponding to a certain gain there is a transient and steady state behavior. If the gain is large the transient is short with the steady state fluctuating error being large. When the gain is small as in the present case there is a large transient with small steady state error. If the filter is run backwards from the end then the whole actual trajectory will be wrapped around by the estimated values. In a nutshell the filter gain values K, can be tuned manually to provide optimal tracking results in a constant gain framework. The filter gain values will be of typical nature as per **Table 5** corresponding to specific target state models. **Figures 9** and **10** illustrate the performance of the CGKF versus the standard KF model. The PFE, RMSPE metrics (as defined in Section 4.1) in the plots correspond to that of the CGKF for a particular run.

4.5 Sensitivity studies on constant gain in case of maneuvering targets (CT (known ω))

Under this heading we demonstrate the robustness of the constant gain in so far as the application of gain variations to the maneuvering target tracking scenario for

MODEL	EKF %	CGKF %	K matrix
CT(known ω)	56.75	10.11	$\begin{pmatrix} .0005 & .0013 \\ .0013 & .0013 \\ .0013 & .0013 \\ .0013 & .0013 \end{pmatrix}$
CT(unknown ω)	24	14.78	$\begin{pmatrix} .0013 & .00007 \\ .0012 & 0 \\ 0 & .0013 \\ .00007 & .0013 \\ .0013 & .0004 \end{pmatrix}$

Table 5.
Percentage fit error comparison:-non linear case and typical K matrix values.

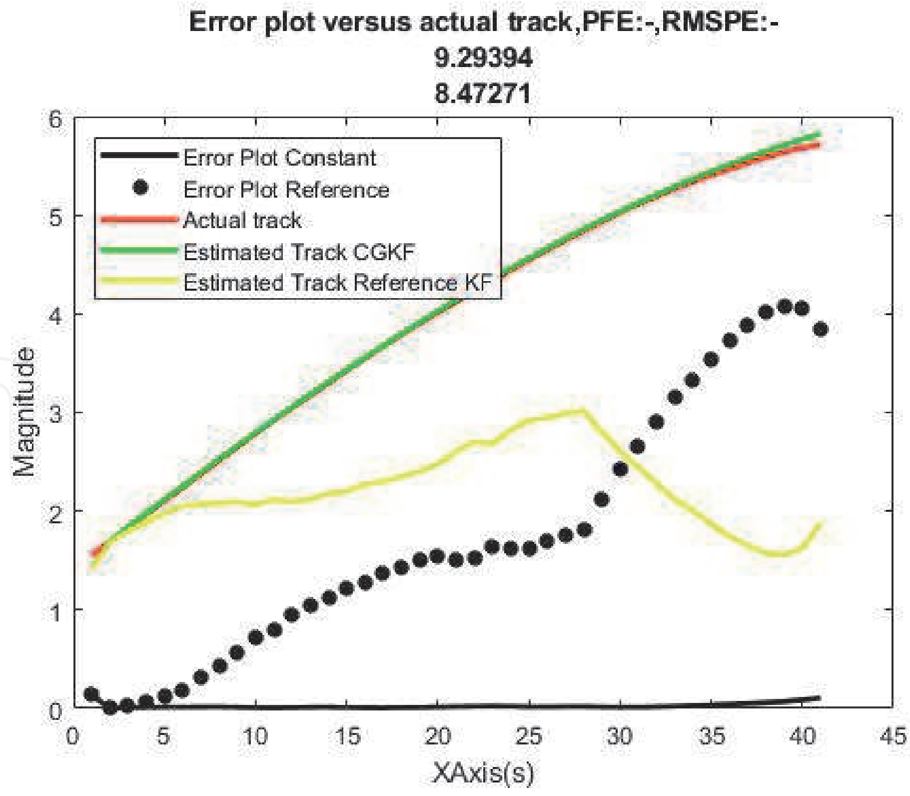

Figure 9.
CT(known ω).

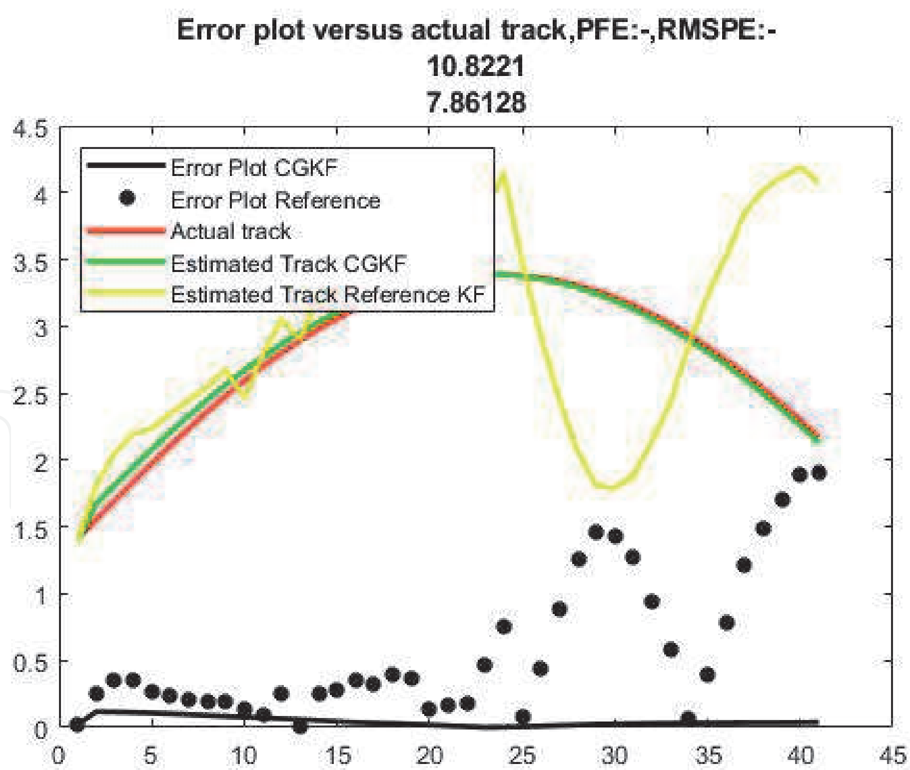

Figure 10.
CT(unknown ω).

the CT (known ω) is concerned. In the tables below are mentioned different PFE/RMSPE metrics achieved as per specified variation in the constant gain values are concerned. In **Table 6** we show variation as per additive increments to the constant gain while in **Table 7** we show variation as per fractional values to the constant gain.

Additive variations (K)	PFE%	RMSPE%
K(1 + .1 randn)	10.9506	13.3848
K(1 + .2 randn)	9.02807	9.8478
K(1 + .3 randn)	11.4343	13.3211
K(1 + .4 randn)	11.4565	13.77
K(1 + .5randn)	8.68005	9.92213
K(1 + .6 randn)	10.3575	10.5219
K(1 + .7 randn)	13.1419	18.0384
K(1 + .8 randn)	10.4037	12.4931

Table 6.
Constant gain robustness to additive variations (CT(known ω)).

Fractional Variations (K)	K/8	K/4	K/2	2 K	4 K	8 K
PFE%	11.1569	9.34031	12.7851	13.0054	11.6087	9.11502
RMSPE%	14.2031	11.0111	15.2803	15.1227	13.0654	10.1699

Table 7.
Constant gain robustness to fractional variations (CT(known ω)).

The tables show that the constant gain is robust to minor additive and fractional increments, thereby demonstrative of the fact that the achieved constant gain provides good tracking results as far as achieved PFE values indicate.

5. Conclusion

We believe that these are the only studies of a CGKF applied to tracking targets in WSN environments and maneuvering target models based on non linear measurement models. As seen the EKF is unable to effectively track the targets in WSN and for the maneuvering target case compared to the CGKF. This is a significant finding and supports the fact that CGKF effectively circumvents, or in other words trades the gains with the filter statistics which are more difficult to obtain and therein gives optimal tracking results by working directly with the Kalman Gain. The present results prove that the CGKF is successful in target tracking applications wherein the constant gain approach overcomes uncertainty regarding noise statistics that exist in the framework of the problem. The CGKF has been employed for tracking maneuvering targets and those in a WSN. The present work firmly establishes the CGKF framework thereby enabling its applicability to a wider variety of problems as deemed fit by the reader.

5.1 Analysis of results and future work

5.1.1 Stand alone mode

Following are the deductions based on the simulation studies as summarized in **Table 2**.

1. The results and plots bring out clearly the novelty of CGKF, the overall performance of which is better than the EKF as per the PFE values.

2. In the case of the EKF the Acoustic sensor performs the best.

3. In case of the CGKF the PIR performs the best.

5.1.2 Homogeneous fusion mode

Following are deductions based on the simulation studies as summarized in **Table 3** [16].

1. The overall performance of the CGKF is better than the EKF for both the MKF and Weighted methods.

2. Considering the CGKF case the PIR and seismic sensors peroform better than the acoustic sensor, with the PIR performing the best overall.

3. Amongst the various fusion methods the overall performance of the weighted fusion is better compared to the MKF, for all types of sensors.

5.1.3 Heterogeneous Fusion mode

Following are the deductions based on the simulation studies as summarized in **Table 4**.

1. Overall the CGKF performance is better than the EKF for heterogeneous fusion method.

2. With reference to heterogeneous fusion of PIR, acoustic and seismic sensors the Durrand Whyte method [24] gives better results compared to Global fusion method [12]. Here we note that a comparison with the CGKF is not possible since the CGKF works with purely measurements and not by propagation of state error covariances which is fundamental to these techniques. The Global fusion method [16] does not provide convergence in tracking when using PIR, acoustic and seismic sensors together.

3. The CGKF heterogeneous fusion model of PIR, Acoustic and seismic sensors gives optimum performance better than its EKF counterpart.

4. PIR based weighted fusion gives better results than the heterogeneous fusion. However we must keep in mind the fact that the simulations for heterogeneous fusion are based only one sensor of each type unlike the homogeneous fusion case where four sensor of each type are considered. The plots and result have been mentioned under. All the result has been obtained through Montecarlo simulation with runs of average of 500.

5.1.4 Maneuvering target

Following are the deductions of the simulations.

1. **Figures 9** and **10** and **Table 5**, clearly show that the performance of the CGKF is very much better than that of the EKF.

2. The results obtained show the CGKF performing better than the EKF in three models (ie. DWPA and both CT models).

3. The results obtained for the CT models including those of sensitivity analysis (Refer **Tables 6** and 7) demonstrates the viability of applying the CGKF to this category of problems.

5.2 Conclusions and Suggestions for Further Studies

The efficacy of the CGKF has been demonstrated wherein a single approach yields optimal results for a varierty of linear [10] as well as non linear models in WSN and maneuvering target scenarios [15]. The extensive numerical studies establish the fact that the CGKF performs better that the conventional EKF.

Actual implementation of a target tracking application in the WSN environment shall require optimal routing, deployment, design, communication protocols and other such associated integral characteristics mentioned in the introduction. Though not directly within the purview of the scope of the work, these aspects are very important.

It would be very useful to apply this CGKF to variants of the Kalman Filter such as particle filter, ensemble filter and other formulations.

Finally CGKF could be tried out for massive data based problems like numerical weather prediction. The constant gains can be pre computed using earlier data and since the gains are robust they can be expected to handle newer data quiet efficiently similar to space debris as in [1].

Author details

Peeyush Awasthi[1], Ashwin Yadav[2*], Naren Naik[3] and Mudambi Ramaswamy Ananthasayanam[4]

1 Graduate Research Scholar, Florida International University, USA

2 Geomatics Engineering, Department of Civil Engineering, Indian Institute of Technology, Roorkee, India

3 Department of Electrical Engineering, Indian Institute of Technology Kanpur, India

4 Department of Aerospace Engineering, Indian Institute of Science, Bangalore, India

*Address all correspondence to: ashwiny77@gmail.com

References

[1] Mudambi R. Ananthasayanam (November 23rd 2018). Tuning of the Kalman Filter Using Constant Gains, Introduction and Implementations of the Kalman Filter, Felix Govaers, IntechOpen, DOI: 10.5772/intechopen.81795. Available from: https://www.intechopen.com/books/introduction-and-implementations-of-the-kalman-filter/tuning-of-the-kalman-filter-using-constant-gains

[2] Mehra, R.K. , “Approaches to adaptive filtering,” in *IEEE Symposium on Adaptive Processes (9th) Decision and Control* , vol.9, no., pp.141, 7-9 Dec. 1970

[3] Robert H Shumway, David S Stoffer; “Time series Analysis and its applications” (Springer Text in Statistics)

[4] Bavdekar, V. A., Deshpande, A. P. and Patwardhan, S. C. (2011) Identification of process and measurement noise covariance for state and parameter estimation using extended Kalman filter. Journal of Process control, 21 : 585-601.

[5] A. H. Mohamed, K. P. Schwartz, “Adaptive Kalman filtering for INS/GPS,” *Journal of Geodesy*, vol 73(2), pp. 193-203,1999.

[6] Myers, K.; Tapley, B.; , “Adaptive sequential estimation with unknown noise statistics,” , *IEEE Transactions on Automatic Control* , vol.21, no.4, pp. 520-523, Aug 1976

[7] R.M.O Gemson and M.R. Ananthasayanam, “Importance of Initial State Covariance Matrix for the parameter estimation using an Adaptive Extended Kalman Filter”,in American Institute of Aeronautics and Astronautics, vol. 4153, pp. 94-104,1998.

[8] Akita, T.; Takaki, R,; Shima, E, “A new adaptive estimation method of spacecraft thermal mathematical model with an ensemble Kalman filter”, Acta Astronautica, vol. 73, April-May 2012, pp 144-155

[9] A.K. Anil Kumar,M.R. Ananthasayanam,P.V. Subba Rao, “A Constant Gain Kalman Filter Approach for the prediction of the re-entry of risk objects”,in *Acta Astronautica* , vol 61 (10), vol-25,pp. 831-839,2007.

[10] Yadav, A.; Naik, N.; Ananthasayanam, M. R.; Gaur, A.; Singh, Y. N., " A constant gain Kalman filter approach to target tracking in wireless sensor networks," Industrial and Information Systems (ICIIS), 2012 7th IEEE International Conference on , vol., no., pp.1,7, 6-9 Aug. 2012

[11] Christian Bohn., “Recursive Parameter Estimation Of Non Linear Continuous-Time Systems through Sensitivity-Model-Based Adaptive Filter”,2000

[12] Jitendra.R.Raol, *Multi Sensor Data Fusion with MATLAB*, CRC Press,2010.

[13] X. Rong Li; Vesselin P Jilkov; , “A Survey of Maneuvering Target Tracking: Dynamic Models”, SPIE conference on Signal and Data processing of small targets, April 2000 (4048-22)

[14] Yaakov Bar-Shalom; Peter K Willet; Xin Tian,*Tracking and datafusion A handbook of algorithms,* YBS Press,2011.

[15] Yadav, A.; Awasthi, P.; Naik, N.; Ananthasayanam, M.R., " A constant gain Kalman filter approach to track maneuvering targets," Control Applications (CCA), 2013 IEEE International Conference on , vol., no., pp.562,567, 28-30 Aug. 2013

[16] R.E Kalman, "A new approach to Linear Filtering and Prediction Problems", in *Transactions of the ASME-Journal of Basic Engineering*, vol. 82, pg-35-45., 1960

[17] Mehra, R.K., " On the Identification of variances and and adaptive Kalman filtering," Automatic Control, IEEE Transactions on , vol. AC-15, No. 2, April 1970

[18] Kailath, T., " An innovations approach to least-squares estimation–Part I: Linear filtering in additive white noise," Automatic Control, IEEE Transactions on , vol.13, no.6, pp.646,655, Dec 1968

[19] Viswanath. Study of constant gain Kalman filter for basic systems with preliminary study of ISAR problem [MTech thesis]. India: IIT Kanpur; 2018

[20] Kalyanmoy Deb, *Multi-Objective Optimization using Evolutionary Algorithms*, Wiley India , 2010.

[21] Nithya V.S.;Sheshadri K; Kumar A; Hari K.V.S; "Model based target tracking in a wireless network of passive infrared sensor nodes" International Conference on Signal Processing and Communications (SPCOM), 2010, 18-21 July 2010

[22] Stefano Coraluppi, Craig Carthel, Mahendra Mallick; "Multi-Target tracking with Unattended Ground Sensors (UGS) Data; ALPHATECH,Inc

[23] H.B.Mitchell; Multi-Sensor Data Fusion, An Introduction 2007

[24] Hugh Durrant-Whyte Lecture notes on "Multi Sensor Data Fusion"

[25] Grimble M J, Jukes K A and D P Goodall, " Nonlinear filters and operators and the constant gain extended Kalman filter," *IMA Journal of Mathematical Control and Inf.*, vol. 1, pp. 359-386, 1984.